





SPECIAL ISSUE ARTICLE

Development of stabilized zirconia–alkali salts dual membranes for carbon dioxide capture

Reginaldo Muccillo  | Sabrina G. M. Carvalho  | Rafael L. Denaldi  |
Eliana N. S. Muccillo 

Energy and Nuclear Research Institute,
Travessa R 400, Cidade Universitária, Sao
Paulo, Sao Paulo, Brazil

Correspondence

Reginaldo Muccillo, Energy and Nuclear
Research Institute, Travessa R 400,
Cidade Universitária, S. Paulo, 05508-170,
SP, Brazil.

Email: muccillo@usp.br

Funding information

CNEN; CDMF-CEPID, Grant/Award
Number: 2013/07296-2; CNPq,
Grant/Award Numbers: 302357/2018-1,
305889/2018-4

Editor's Choice

The Editor-in-Chief recommends this
outstanding article.

Abstract

Molten $\text{Na}_2\text{CO}_3\text{--K}_2\text{CO}_3$ (NKC, 56–44 mol%) eutectic compositions were vacuum-impregnated, at the eutectic temperature, into two porous $\text{ZrO}_2\text{:}8.6$ mol% MgO (magnesium-partially stabilized zirconia, MgPSZ) and $\text{ZrO}_2\text{:}8$ mol% Y_2O_3 (yttria-fully stabilized zirconia, 8YSZ) ceramics. Thermogravimetric analyses were performed in mixtures of that composition with MgPSZ and 8YSZ ceramic powders. Before impregnation, porosity was achieved in the two compounds by addition and thermal removal of 30 vol.% NKC. To ascertain the carbonates had filled up through the ceramic body, both sides of the parallel and fracture surfaces of the disk-shaped impregnated compositions were observed in a scanning electron microscope and analyzed by energy-dispersive X-ray spectroscopy. The electrical conductivity of the two ceramics, before and after impregnation, was evaluated by electrochemical impedance spectroscopy in the 5 Hz–13 MHz frequency range from approximately 530 to 740°C. The permeation of the carbonate ions through the membranes via the eutectic composition was assessed by the threshold temperatures of the onset of the carbonate ion percolation. The objectives were to prepare dual-phase membranes for the separation of carbon dioxide and for the development of carbon dioxide sensors.

KEYWORDS

carbon dioxide permeation, ceramic membranes, impedance spectroscopy, scanning electron microscopy, stabilized zirconia

1 | INTRODUCTION

Overall, 56 mol% Na_2CO_3 (M.P. 854°C) and 44 mol% K_2CO_3 (891°C) constitute a eutectic composition that melts at 710°C.¹ At that temperature, CO_3^{2-} ions are the mobile charge carriers under an electric field. Hence, oxide ion conducting ceramic mixed to that eutectic compound, with improved electrical conductivity, was proposed as high-temperature membranes for carbon dioxide separation or capture, and also as solid electrolytes in solid

oxide fuel cells for alternative electric energy supply.^{2–9} The dual-phase membranes for carbon dioxide capture were composed of a solid electrolyte matrix, mainly gadolinium-doped ceria or samarium-doped ceria, mixed to or impregnated with eutectic compositions of alkali halide carbonates, for example, $(\text{Li}_2, \text{Na}_2)\text{CO}_3$,^{10–13} $(\text{Li}_2, \text{K}_2)\text{CO}_3$,¹⁴ or $(\text{Li}_2, \text{Na}_2, \text{K}_2)\text{CO}_3$.^{13,15,16–21} The melting points of 56 mol% $\text{Na}_2\text{CO}_3\text{--}44$ mol% K_2CO_3 , 52 mol% $\text{Li}_2\text{CO}_3\text{--}48$ mol% Na_2CO_3 , 62 mol% $\text{Li}_2\text{CO}_3\text{--}38$ mol% K_2CO_3 , and 43.5 mol% $\text{Li}_2\text{CO}_3\text{--}31.5$ mol% $\text{Na}_2\text{CO}_3\text{--}25$ mol% K_2CO_3 eutectic

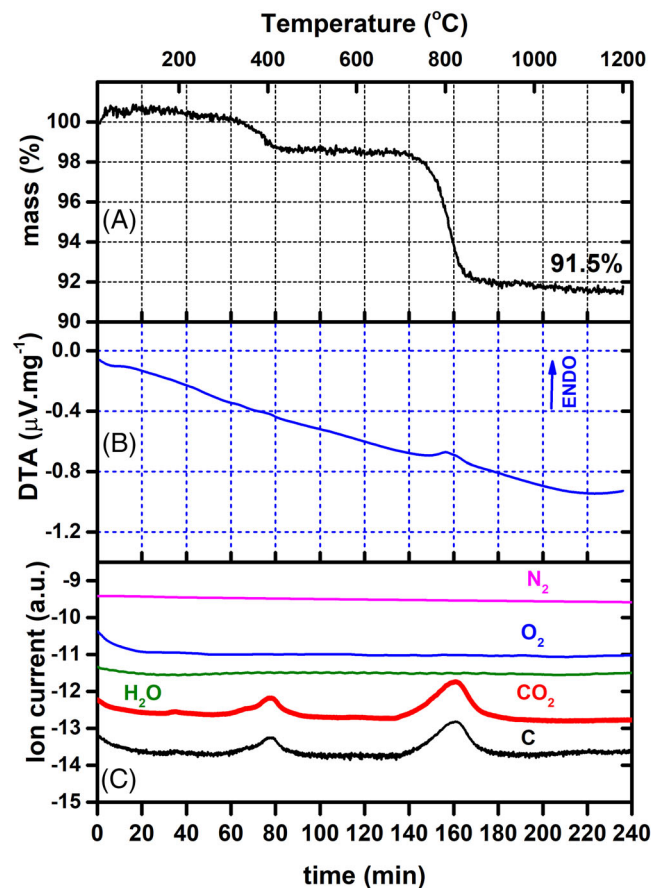


FIGURE 1 Thermogravimetric (A) and differential thermal analysis (B) curves of MgPSZ (ZrO_2 :8.6 mol% MgO) ceramic powders mixed to 30 vol.% of NKC (56 mol% Na_2O_3 –44 mol% K_2CO_3); (C) simultaneous mass spectrometric relative data of N_2 , O_2 , H_2O , CO_2 , and C. N_2 was the sweeping gas.

compositions are 710, 501, 498, and 397°C, respectively.¹ MgPSZ was also reported as oxygen ion conducting solid electrolyte matrix.²²

The mechanism involved in the CO_2 separation membranes is based on carbonate and oxide ions transport through the membrane, both O^{2-} and CO_3^{2-} ions in counter flow motions, resulting in net CO_2 transport.¹⁵ The oxygen ion conductivity is lower than the carbonate ion conductivity at the temperature of the molten carbonates.^{23,24} Percolation of the carbonate ions is achieved by a suitable composition of the two-phase membranes, allowing for a surface-to-surface ionic conductivity in disk-shaped membranes.

Several methods have been used for the fabrication of porous ceramics: polymer derived,²⁵ gelation-freezing,²⁶ direct foaming,²⁷ tape casting,²⁸ freeze casting,²⁹ and spark plasma sintering.³⁰

The aim of this work was to study carbon dioxide ions motion in molten sodium–potassium carbonates through two oxygen ion conductors as ceramic matrices:

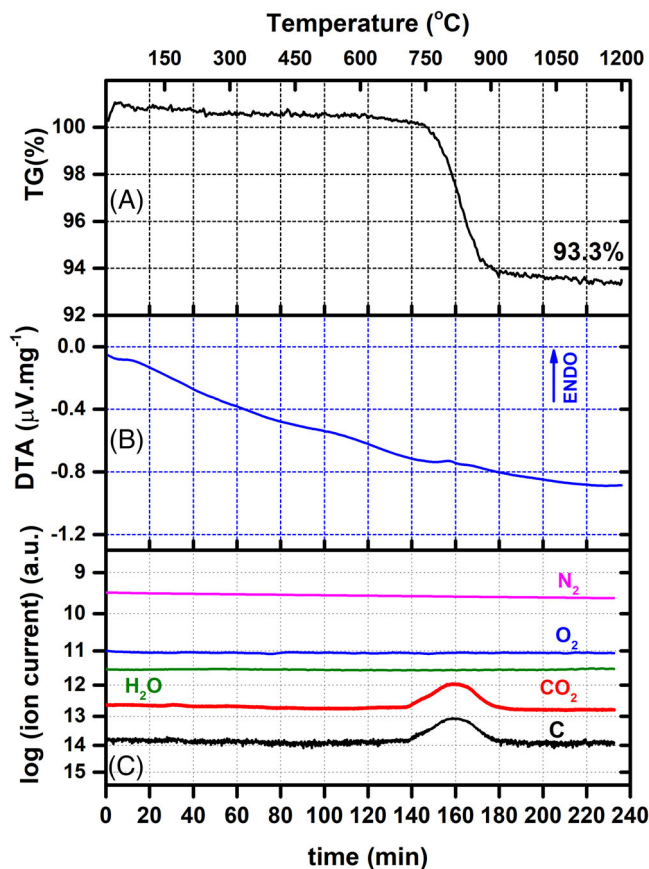


FIGURE 2 Thermogravimetric (A) and differential thermal analysis (B) curves of 8 mol% yttria-stabilized zirconia (8YSZ) (ZrO_2 :8 mol% Y_2O_3) ceramic powders mixed to 30 vol.% of NKC (56 mol% Na_2O_3 –44 mol% K_2CO_3); (C) simultaneous mass spectrometric relative data of N_2 , O_2 , H_2O , CO_2 , and C. N_2 was the sweeping gas.

zirconia:8.6 mol% magnesia (MgPSZ) and zirconia:8 mol% yttria-stabilized zirconia (8YSZ). MgPSZ is a well-known toughened ceramic material with enhanced thermomechanical properties, being used mainly in disposable high-temperature oxygen sensors in steel production^{31–33}; 8YSZ is a well-utilized ceramic material with oxygen ion conductivity appropriate to use either as an oxygen sensor in automotive vehicles for improving engine efficiency and fuel economy,³² or as solid electrolyte in high-temperature solid oxide fuel cells for alternative electrical energy production.³⁴

2 | MATERIALS AND METHODS

The starting materials were magnesia-partially stabilized zirconia (MSZ-8 MgPSZ, ZrO_2 :8.6 mol% MgO, DKKK Co., Ltd., Japan, 3–6 m^2/g specific surface area, .6–2.0 μm average particle size),³⁵ YSZ (8YSZ, ZrO_2 :8 mol% Y_2O_3 , Fuel Cell Materials, USA, 6–9 m^2/g , .5–.7 μm),³⁶ sodium

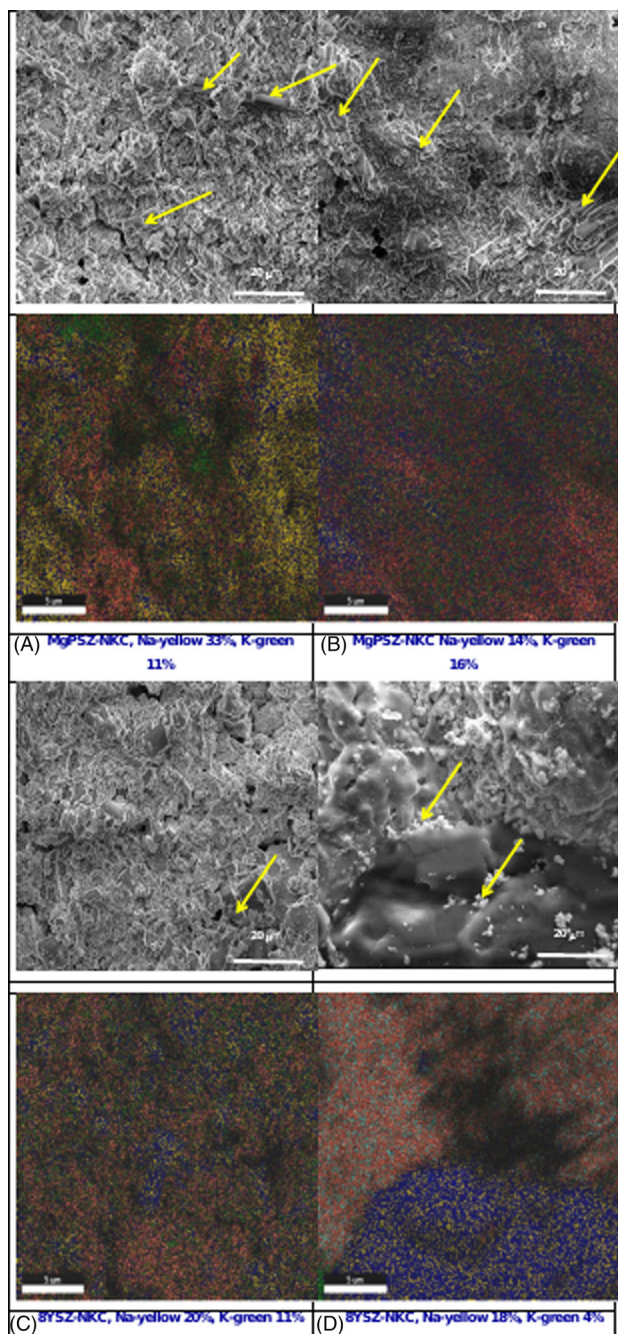


FIGURE 3 Scanning electron microscopy micrographs (top) and elemental EDX mapping (bottom) of both surfaces of (A and B) ZrO_2 :8.6 mol% MgO and (C and D) ZrO_2 :8 mol% Y_2O_3 ceramic membranes impregnated with 30 vol.% (56 mol% Na_2CO_3 –44 mol% K_2CO_3); the relative amounts of sodium (yellow) and potassium (green) are shown; arrows point to the carbonate phase.

carbonate (anhydrous Na_2CO_3 , 99.5% min, Alfa Aesar), and potassium carbonate (anhydrous K_2CO_3 , 99%, Alfa Aesar). All compounds were analyzed by X-ray diffraction (D8 Advance, Bruker AXS diffractometer, Karlsruhe, Germany) in Bragg–Brentano configuration, $\text{Cu-}k_\alpha$ radiation, 20° – 80° 2θ range, $.05^\circ$ 2θ step size, and 5 s/step. For the

preparation of MgPSZ and 8YSZ porous matrices, those powders were individually mixed to 1.0 wt.% polyvinyl alcohol and a eutectic composition of sodium and potassium carbonates (56 mol% Na_2CO_3 –44 mol% K_2CO_3), ball milled at 5000 rpm during 2 h with 1 mm diameter TZP zirconia medium in isopropyl alcohol inside a custom-made attritor. These powders were uniaxially cold-pressed under 30 MPa and then isostatically (National Forge Co., Irvine, PA, USA) under 200 MPa to $\phi 12$ mm \times 2 mm thickness pellets. The pellets were heated inside alumina crucibles at $2^\circ/\text{min}$ to $720^\circ\text{C}/2$ h for wetting the matrix particles with the molten eutectic composition afterward were heated to $1450^\circ\text{C}/2$ h at $5^\circ/\text{min}$ to remove that composition by evaporation and finally cooled down at $5^\circ/\text{min}$ to room temperature. The porous matrices were impregnated with the eutectic composition in a custom-made apparatus, consisting of an L-shaped quartz tube with an end connected to a vacuum pump and the other end to the porous matrix; the porous matrix was fixed with an alcoholic solution of the matrix powder and coated with a powder mixture of the eutectic carbonate composition; the quartz tube with the upright-positioned coated matrix was inserted into a resistive furnace programed to be heated to 720°C , to melt the eutectic composition. At that temperature, the other end of the quartz tube, located outside the furnace, was pumped out with several 1 s pulses to help the molten eutectic composition to fill up the pores of the ceramic matrix; the furnace is then switched off.

Thermogravimetric analyses were carried out in MgPSZ and 8YSZ powders after thoroughly mixing with 30 vol.% of the eutectic composition of NKC (56 mol% Na_2CO_3 –44 mol% K_2CO_3), and also in NKC powders. The measurements were performed in a Netzsch 409 E equipment (Selb, Germany) from room temperature to 1200°C with $5^\circ\text{C}/\text{min}$ heating and cooling rates. A dynamic 10 ml/min flow of synthetic nitrogen was used. A mass spectrometer (Thermostar GSD 350 T, Pfeiffer Vacuum, Asslar, Germany) was connected to the gas outlet of the thermogravimetric equipment to analyze the outflow of gaseous species during heating.

The parallel and fracture surfaces of the as-prepared eutectic carbonates-impregnated ceramic pellets were observed in a scanning electron microscope (FEG-SEM Inspect F50, Brno, Czech Republic), operating at 5 kV and 3.5 spot size. The FEG-SEM was equipped with an energy-dispersive spectrometer (Octane Elect Plus, EDAX, Ametek, USA), operating at 20 kV and 5.0 spot size.

For the impedance spectroscopy measurements, platinum paste (Degussa Demetron 308A, Hanau, Germany) was brush painted on the parallel surfaces of the eutectic carbonates-impregnated ceramic pellets (hereafter membranes) for the analysis of their electrical behavior at

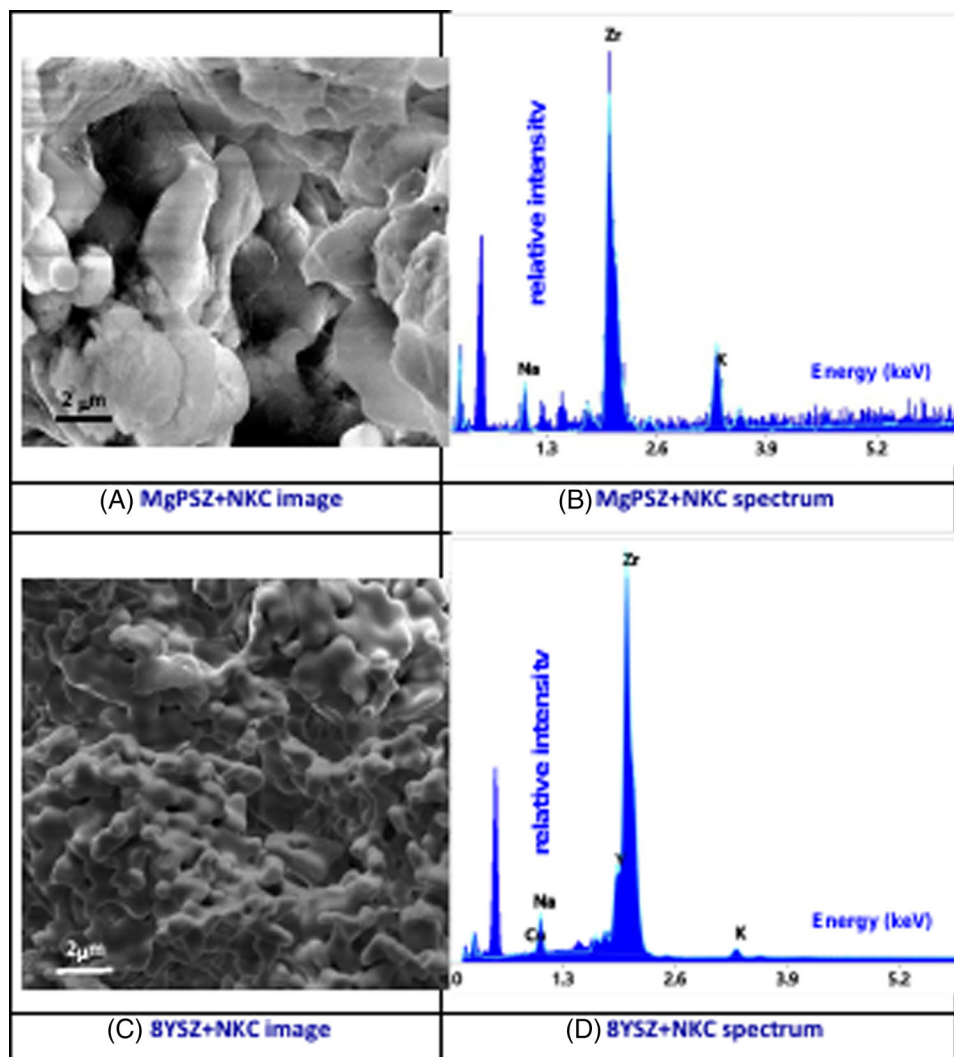


FIGURE 4 Images and EDS spectra of fracture surfaces of (A and B) ZrO_2 :8.6 mol% MgO and (C and D) ZrO_2 :8 mol% Y_2O_3 porous ceramics impregnated with 30 vol.% of 56 mol% Na_2CO_3 –44 mol% K_2CO_3

temperatures below and above the eutectic temperature of the sodium–potassium carbonates. Electrical measurements were carried out with a 4192A Hewlett Packard impedance analyzer connected to a series 360 Hewlett Packard controller, applying 200 mV input AC signal in the 5 Hz–4.7 MHz frequency range from 470 to 740°C. The $[-Z''(\omega) \times Z'(\omega)]$ data, $\omega = 2\pi f$, f is the frequency of the input signal, were collected and deconvoluted for the evaluation of the total electric resistivity with a special software.³⁷ For these measurements, each sample was spring-loaded with platinum disks inside an alumina sample holder, which was inserted in a programmable furnace and connected to the impedance analyzer with a test fixture (Hewlett Packard 16047C). A type K chromel–alumel thermocouple with its tip positioned close to the ceramic membrane was used to monitor the sample temperature.

3 | RESULTS AND DISCUSSION

3.1 | Thermal analysis

Figures 1 and 2 show thermogravimetric and differential thermal analyses of 30 mg of a mixture of MgPSZ and 8YSZ with NKC under the following conditions: RT–1200°C, 5°C/min, and 10 ml/min N_2 flux along with mass spectrometer data. The composition with MgPSZ matrix showed mass losses in the 300–400 and 700–800°C ranges, simultaneous to carbon dioxide and carbon detection with the mass spectrometer. The mass loss in the first temperature range might be due to a decomposition of magnesium carbonate producing magnesium oxide and carbon dioxide³⁸; the mass loss in the second range is due probably to after-melting decomposition of the carbonates. The composition with 8YSZ matrix showed mass loss only

in the 700–900°C range with outflows of carbon dioxide, similar to MgPSZ behavior. The total mass losses were 8.5% and 6.7% for the MgPSZ- and 8YSZ-based compositions, respectively.

The differential thermal analyses show an endothermic peak centered at approximately 800°C, corresponding to the decomposition of NKC.

3.2 | Microstructural analysis

SEM micrographs of both top and bottom surfaces of the ceramic membranes are shown in Figure 3 the arrows pointing to the location of the carbonates. The images of the carbonate phase are typical of a composition that passed to a molten phase, spreading in the ceramic matrix before solidifying. The presence of carbonates in both parallel faces of the ceramic membrane shows that the pores crossed the membrane thickness, allowing for the percolation of the carbonate phase. Even though the uneven distribution of the elements, the EDX images were important to show sodium and potassium in both parallel faces of the cylindrical pellets, assuring that the high-temperature vacuum-impregnation was efficient.

Fracture surface images of ZrO_2 :8.6 mol% MgO and ZrO_2 :8 mol% Y_2O_3 porous ceramics impregnated with 30 vol.% of the eutectic composition were also observed in the SEM. Additional EDX analysis was carefully performed searching for Na or K. Figure 4A,C shows the images and (B) and (D) the EDX spectra of both samples.

Despite the difficulty of detecting low Z elements, Na and K were detected in both fracture surfaces of MgPSZ and 8YSZ porous ceramics impregnated with sodium-potassium carbonates.

The software ImageJ³⁹ was adopted for the evaluation of the average pore size, by analyzing different areas of the SEM micrographs. These values were 6.0 and 1.5 μm^2 for MgPSZ and 8YSZ porous ceramics, respectively.

3.3 | Impedance spectroscopy analysis

Figure 5A–C shows $[-Z''(\omega) \times Z'(\omega)]$ impedance spectroscopy diagrams of the two ceramic membranes and of the eutectic composition upon heating to several temperatures in the 530–740°C range, waiting for 30 min to stabilize the set temperature and collecting the impedance data from 5 Hz to 4.7 MHz. The impedance diagrams of MgPSZ-NKC ceramic pellets present only one semicircle arc in the whole frequency range, the electrical resistance decreasing up to temperatures close to the melting point of the eutectic carbonate mixture. The impedance diagram of the 8YSZ-NKC ceramic pellet, on the other hand,

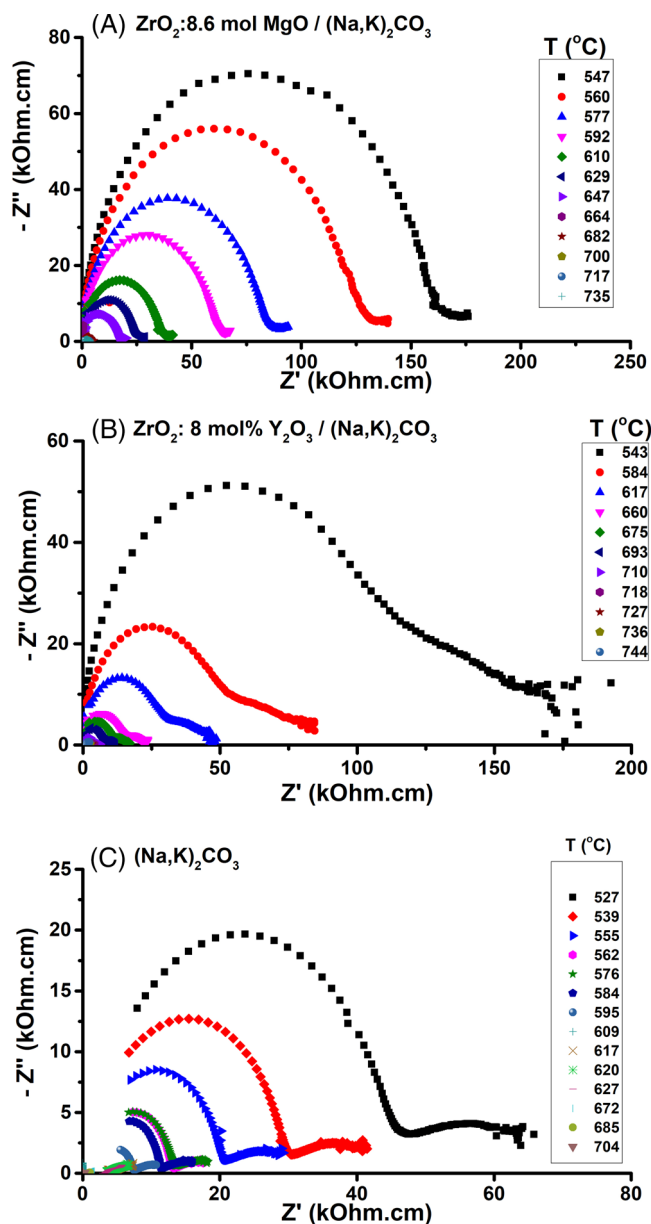


FIGURE 5 Impedance spectroscopy diagrams of (A) ZrO_2 :8.6 mol% MgO and (B) ZrO_2 :8 mol% Y_2O_3 ceramic membranes impregnated with 30 vol.% (56 mol% Na_2CO_3 –44 mol% K_2CO_3) at several temperatures; (C) 56 mol% Na_2O_3 –44 mol% K_2CO_3

apparently presents two semicircle arcs, the total resistance decreasing as well up to temperatures close to the melting point of the eutectic carbonate mixture. All those behaviors of the electrical resistance of the ceramic membranes are shown in Figure 6.

Figure 6 shows the Arrhenius plots of the electrical resistivity of the two ceramic membranes and also of the NKC pellet. The values of the electrical resistance were taken at the intersection of the semicircle arc at the low-frequency side of the impedance diagram and corrected for the geometrical factor (area of the electrodes/thickness

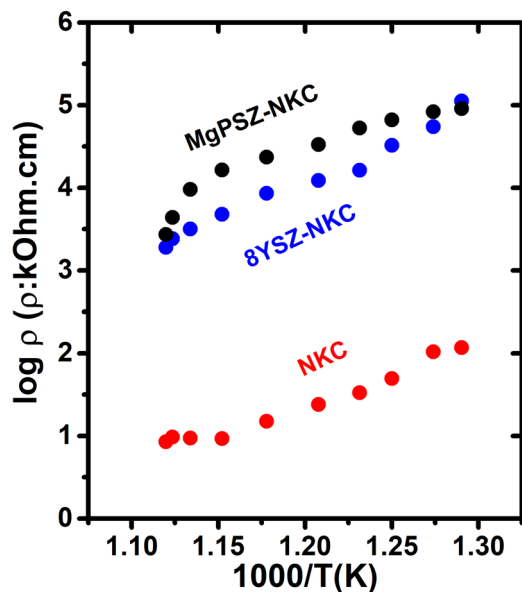


FIGURE 6 Arrhenius plots of the electrical resistivity of 8 mol% yttria-stabilized zirconia (8YSZ)-NKC and MgPSZ-NKC ceramic membranes. NKC impregnation content = 30 vol.%. 8YSZ = ZrO_2 :8.0 mol% Y_2O_3 , MgPSZ = ZrO_2 :8.6 mol% MgO, NKC = 56 mol% Na_2CO_3 -44 mol% K_2CO_3

of the sample). The behavior of all curves is the same, that is, a decrease of the resistivity for increasing temperature, reaching similar values at 710°C, the melting point of the sodium-potassium carbonate eutectic composition, when the electrical conductivity of the carbonate ions prevails over that of the zirconia-based solid electrolytes. The electric current through the porous matrices impregnated with sodium-potassium carbonates is described as $j_{\text{carbonates}} + j_{\text{matrix}}$, the former predominating in the molten carbonates.

Figure 7 shows results of the electrical measurements performed at the same temperature (590°C) of MgPSZ and 8YSZ samples with and without impregnation with sodium-potassium carbonates. The contribution of the carbonates to the total electrical resistivity is evident. MgPSZ had a total electrical resistivity >1.0 MΩ cm, whereas for the alkali salt-impregnated MgPSZ, the total resistivity was 65.7 kΩ cm. For 8YSZ, these figures were >273 and 85.8 kΩ cm. As expected, the ionic conductivity of 8YSZ⁴⁰ is higher than that of MgPSZ.⁴¹

4 | CONCLUSIONS

Magnesia-partially stabilized zirconia (MgPSZ) and yttria fully stabilized zirconia (8YSZ) porous ceramics were successfully obtained by the addition and thermal removal of the eutectic composition of sodium and potassium

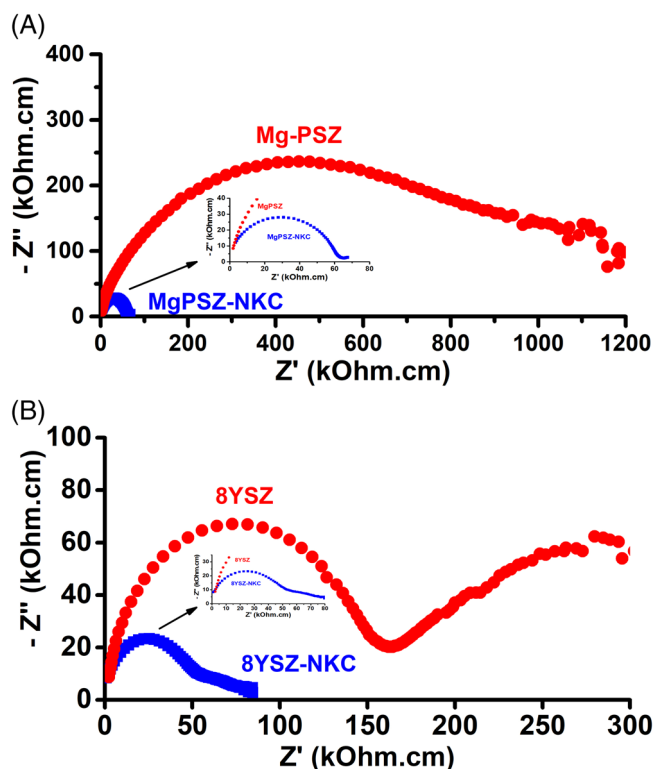


FIGURE 7 Impedance spectroscopy diagrams at 590°C of porous and impregnated (with 56 mol% NaCO_3 -44 mol% K_2CO_3) ceramics. (A) ZrO_2 :8.6 mol% MgO (MgPSZ) and (B) ZrO_2 :8 mol% Y_2O_3

carbonates. Mass spectrometer analysis, simultaneous to thermogravimetric and differential thermal analyses of those solid electrolytes mixed to the eutectic composition, identified the temperatures carbon dioxide evolved from the mixtures. Two-phase membranes were obtained by high-temperature vacuum impregnating those porous matrices with the molten eutectic composition. With EDX analysis, sodium and potassium were detected at both parallel surfaces and at fracture surfaces of the disk-shaped ceramic membranes. The percolation of carbonate ions was monitored by the impedance spectroscopy technique up to 740°C. At 710°C, the melting point of the eutectic carbonates composition, the electrical conductivity of the carbon dioxide ion was shown to predominate over the electrical conductivity of the membrane matrices. For the preparation of solid electrolyte/alkali carbonates membranes, it is proposed the use of the alkali carbonates as sacrificial pore former; the advantage was the wetting of the solid electrolyte grains, offsetting the negative impact of the fouling effect.

AUTHOR CONTRIBUTIONS

Design; experimentation; analysis; writing; approval: Reginaldo Muccillo (leader, advisor). *Experimentation:*

Sabrina G. M. Carvalho, Rafael L. Denaldi (contributor). *Experimentation; analysis; writing*: Eliana N. S. Muccillo (contributor).


ACKNOWLEDGMENT

Dr. S.G.M. Carvalho and R.L. Denaldi acknowledge Shell and CAPES, respectively, for the scholarships. This work was supported by CNEN, CDMF-CEPID (FAPESP Proc. 2013/07296-2), and CNPq (Procs. 302357/2018-1, 305889/2018-4).

CONFLICT OF INTEREST

The authors state that there is no conflict of interest.

ORCID

Reginaldo Muccillo  <https://orcid.org/0000-0002-8598-279X>

Sabrina G. M. Carvalho  <https://orcid.org/0000-0003-2766-3173>

Rafael L. Denaldi  <https://orcid.org/0000-0001-6936-5110>

Eliana N. S. Muccillo  <https://orcid.org/0000-0001-9219-388X>

REFERENCES

- Frangini S, Masi A. Molten carbonates for advanced and sustainable energy applications: Part I. Revisiting molten carbonate properties from a sustainable viewpoint. *Int J Hydrogen Energy*. 2016;41:18739–46.
- Zhang P, Tong J, Huang K, Zhu X, Yang W. The current status of high temperature electrochemistry-based CO₂ transport membranes and reactors for direct CO₂ capture and conversion. *Prog Energy Combust Sci*. 2021;82:100888.
- Zhu B, Liu XR, Zhou P, Zhu ZG, Zhu W, Zhou SF. Cost-effective yttrium doped ceria-based composite ceramic materials for intermediate temperature solid oxide fuel cell applications. *J Mater Sci Lett*. 2001;20:591–4.
- Zhu B, Yang XT, Xu J, Zhu ZG, Ji SJ, Sun MT, et al. Innovative low temperature SOFCs and advanced materials. *J Power Sources*. 2003;118:47–53.
- Zhu B. Functional ceria-salt-composite materials for advanced ITSOFC applications. *J Power Sources*. 2003;114:1–9.
- Chen M, Zhang H, Fan L, Wang C, Zhu B. Ceria-carbonate composite for low temperature solid oxide fuel cell: sintering aid and composite effect. *Int J Hydrogen Energy*. 2014;39:12309–16.
- Liangdong F, Chuanxin H, Zhu B. Role of carbonate phase in ceria-carbonate composite for low temperature solid oxide fuel cells: a review. *Int J Energy Res*. 2017;41:465–81.
- Benamira M, Ringuedé A, Hildebrandt L, Lagergren C, Vannier R-N, Cassir M. Gadolinia-doped ceria mixed with alkali carbonates for SOFC applications: II An electrochemical insight. *Int J Hydrogen Energy*. 2012;37:19371–9.
- Ali SAM, Muchtar A, Sulong AB, Muhamad N, Majlan EH. Influence of sintering temperature on the power density of samarium-doped-ceria carbonate electrolyte composites for low-temperature solid oxide fuel cells. *Ceram Int*. 2013;39:5813–20.
- Rondão AIB, Patrício SG, Figueiredo FML, Marques FMB. Impact of ceramic matrix functionality on composite electrolytes performance. *Electrochim Acta*. 2013;109:701–9.
- Yang Z, Zhu Y, Han M. Synthesis and characterization of gadolinium doped ceria-carbonate dual-phase membranes for carbon dioxide separation. *J Alloys Compd*. 2017;723:70–4.
- Dilimon VS, Strandbakke R, Norby T. Impedance spectroscopy study of Au electrodes on Gd-doped CeO₂ (GDC)-molten Li₂CO₃+Na₂CO₃ (LNC) composite electrolytes. *J Power Sources*. 2022;522:230986.
- Li Y, Rui Z, Xia C, Anderson M, Lin YS. Performance of ionic-conducting ceramic/carbonate composite material as solid oxide fuel cell electrolyte and CO₂ permeation membrane. *Catal Today*. 2009;148:303–9.
- Yang L, Ricote S, Lundin STB, Way JD. Ceramic/metal-supported, tubular, molten carbonate membranes for high-temperature CO₂ separations. *Ind Eng Chem Res*. 2020;59:13706–15.
- Wade JL, Lee C, West AC, Lackner KS. Composite electrolyte membranes for high temperature CO₂ separation. *J Membr Sci*. 2011;369:20–9.
- Norton TT, Lu B, Lin YS. Carbon dioxide permeation properties and stability of samarium-doped-ceria carbonate dual-phase membranes. *J Membr Sci*. 2014;467:244–52.
- Lu B, Lin YS. Asymmetric thin samarium doped cerium oxide-carbonate dual-phase membrane for carbon dioxide separation. *Ind Eng Chem Res*. 2014;53:13459–66.
- Xia C, Li Y, Tian Y, Liu Q, Zhao Y, Jia L, et al. A high performance composite ionic conducting electrolyte for intermediate temperature fuel cell and evidence for ternary ionic conduction. *J Power Sources*. 2009;188:156–62.
- Papaioannou EI, Qi H, Metcalfe IS. 'Uphill' permeation of carbon dioxide across a composite molten salt-ceramic membrane. *J Membr Sci*. 2015;485:87–93.
- Grilo JPF, Macedo DA, Nascimento RM, Marques FMB. Electronic conductivity in Gd-doped ceria with salt additions. *Electrochim Acta*. 2019;318:977–88.
- Nikolaeva EV, Bovet AL, Zakiryanova ID. Electrical conductivity of molten carbonate and carbonate-chloride systems coexisting with aluminum oxide powder. *Z Naturforsch*. 2018;73:79–83.
- Grima L, Mutch GA, Oliete PB, Bucheli W, Merino RI, Papaioannou EI, et al. High CO₂ permeability in supported molten-salt membranes with highly dense and aligned pores produced by directional solidification. *J Membr Sci*. 2021;630:119057.
- Wade JL, Lackner KS, West AC. Transport model for a high temperature, mixed conducting CO₂ separation membrane. *Solid State Ionics*. 2007;78:1530–40.
- Rui ZB, Anderson M, Lin YS, Li YD. Modeling and analysis of carbon dioxide permeation through ceramic-carbonate dual-phase membranes. *J Membr Sci*. 2009;345:110–8.
- Vakifahmetoglu C, Zeydanli D, Colombo P. Porous polymer derived ceramics. *Mater Sci Eng R – Rep*. 2016;106:1–30.
- Fukushima M, Yoshizawa Y, Ohji T. Macroporous ceramics by gelation-freezing route using gelatin. *Adv Eng Mater*. 2014;16:607–20.
- Shimamura A, Fukushima M, Hotta M, Ohji T, Kondo N. Fabrication and characterization of porous alumina with denser surface layer by direct foaming. *J Ceram Soc Jpn*. 2017;125:7–11.

28. Nishihora RK, Rachadel PL, Quadria MGN, Hotza D. Manufacturing porous ceramic materials by tape casting – a review. *J Eur Ceram Soc.* 2018;38:988–1001.
29. Zhang Y, Wang N, Du Y, Shi X, Wang WC, Zhang JZ. Research progress in porous ceramics prepared by freeze casting. *J Mater Eng.* 2019;47:26–34.
30. Dudina DV, Bokhonov BB, Olevsky EA. Fabrication of porous materials by spark plasma sintering: a review. *Materials.* 2019;12:541.
31. Stevens R. Zirconia and zirconia ceramics. Manchester, UK: Magnesium Elektron Ltd; 1986. Publ. No. 113.
32. Jagannathan KP, Tiku SK, Ray HS, Ghosh A, Subbarao EC. Technological applications of solid electrolytes. In: Subbarao EC, editor. *Solid electrolytes and their applications.* Boston, MA, USA: Springer; 1980. p. 201–59.
33. Rondão AIB, Muccillo ENS, Muccillo R, Marques FMB. On the electrochemical properties of Mg-PSZ: an overview. *J Appl Electrochem.* 2017;47:1091–113.
34. Goodenough JB. Oxide-ion electrolytes. *Ann Rev Mater Res.* 2003;33:91–128.
35. Available from: Complex Oxide <https://www.dkkk.co.jp/english/products/pro03.html>
36. fuelcellmaterials.com/products/powders/electrolyte-powders/electrolyte-yttria-stabilized/yttria-stabilized-zirconia-8-y-tape-cast-grade-powder/
37. Kleitz M, Kennedy JH. Resolution of multicomponent impedance diagrams. In: Mundy JN, Shenoy GK, Vashishta P, editors. *Fast ion transport in solids.* North Holland: Elsevier; 1979. p. 185–8.
38. CRC Handbook of Chemistry and Physics. CRC Press: West Palm Beach, FL, USA; 2014–2015. p. B-133. Available from: https://en.wikipedia.org/wiki/Magnesium_carbonate
39. <https://imagej.nih.gov/ij/>
40. Etsell TH, Flengas SN. The electrical properties of solid oxide electrolytes. *Chem Rev.* 1970;70:339–76.
41. Wen T, Li X, Kuo C, Weppner W. Conductivity of MgO-doped ZrO₂. *Solid State Ionics.* 1986;18–19:715–9.

How to cite this article: Muccillo R, Carvalho SGM, Denaldi RL, Muccillo ENS. Development of stabilized zirconia–alkali salts dual membranes for carbon dioxide capture. *Int J Appl Ceram Technol.* 2023;20:951–958. <https://doi.org/10.1111/ijac.14290>